Minimizing Quench Distortion and Improving the Toughness of Complex Hollow Extrusions Using Internal Cooling

Ala'aldin Alafaghani, Lillian Adams, Pingsha Dong, and Daniel Cooper(✉)

University of Michigan, Ann Arbor, MI 48109, USA
drcooper@umich.edu

Abstract. Lightweight automotive extrusions are increasingly complex, thin-walled, multi-hollow profiles made from high-strength, quench-sensitive aluminum alloys such as AA6082. These alloys require rapid quenching as the profile leaves the press to prevent the precipitation of undesired phases, to create a supersaturated solid solution, and to prepare them for subsequent age-hardening treatments; e.g., for the T6 temper. However, rapid quenching can cause profile distortion, which leads to high scrap reject rates, increasing costs, environmental impacts, and production lead time. This study tests two hypotheses: (1) That the different cooling rates set-up across the profile section during quenching induces not only distortion but also varying mechanical properties across the section; and (2) That this temperature differential can be minimized by combining (conventional) external quenching with internal quenching supplied by through-die cooling channels. The first hypothesis is tested experimentally by taking tensile specimens from different locations of an AA6082 multi-hollow profile, showing a significant decrease in the ductility and ultimate tensile strength of samples extracted from internal webs. The second hypothesis is tested by performing thermo-mechanical finite element simulations that compare the thermal history, stresses, and strains of simultaneous internal and external quenching in contrast with conventional quenching (external only). The combined quenching approach results in a significant reduction in the residual stress and plastic deformation. This implies lower scrap reject rates, improved internal wall mechanical properties (giving scope for further light-weighting), and a wider profile design space by enabling the extrusion of more challenging profile shapes.

Keywords: Aluminum · Automotive · Lightweighting · Residual Stress

1 Introduction

Lightweighting has been a major automotive industry objective in recent years. This led to the rapid and continuing expansion of the aluminum extrusion transport sector [1]. Applications include roof bows, front end and roof structures, multi-hollow rocker and engine cradle components, battery housing, and crash management systems. Therefore, OEMs are pursuing aluminum extrusions with thinner walls, more complex hollow profiles, and stronger alloys to improve structural efficiency [2, 3].

K. Mocellin et al. (Eds.): ICTP 2023, LNME, pp. 531–543, 2024.
https://doi.org/10.1007/978-3-031-41023-9_54

The AA6xxx series is one of the most common alloys used in the automotive and aerospace industries [4] due to their satisfactory strength combined with their excellent corrosion resistance. The AA6xxx series alloys are heat-treatable alloys that can be strengthened by precipitation during artificial aging. One of the most commonly used aging cycles for aluminum is the T6 temper in which, normally, the alloy is solution treated, quenched, and aged to peak strength at a suitable elevated temperature [5]. For extruded aluminum, however, the solution annealing heat treatment is skipped. This requires that the temperature of the workpiece be above the solvus temperature during the extrusion to maintain the alloying elements in a solution condition followed by rapid profile cooling to prevent undesired precipitation. This followed by the appropriate aging treatment satisfies the requirements of T6 temper according to footnote 9 in Aluminum Standards and Data [6]. The tensile strength, ductility, and crush rating of artificially aged quench-sensitive alloys such as AA6061 and AA6082 are highly dependent on the press-quench cooling rate. These quality metrics are dramatically reduced with cooling rates below 10 °C/s [7]. In this work, we will focus on AA6082 as it has been increasingly replacing the AA6061 in the automotive industry due to its superior strength and weldability.

AA6082 is characterized by its composition, 0.4–1% Mn, 0.6–1.2 Mg, 0.7–1.3 Si, traces of other metals, and ~97% Al [8, 9]. The Mg and Si play a significant role in strengthening the alloy. The Mg and Si supersaturating the solid solution alloy start clustering and forming GP zones during T6 tempering. The GP zones then form β'' precipitates which can transform to β' and the stable phase β if the artificial aging treatment is prolonged. The precipitate evolution is usually described in the literature as follows: of Si atoms $\rightarrow$ GP I zones $\rightarrow$ GP II zones/β'' $\rightarrow$ β' $\rightarrow$ β [10, 11]. Greater amounts of β'' precipitates are desired for their superior strengthening effect on the alloy due to the coherency of β'' with the matrix [12–14]. Overaged AA6082 contains larger precipitates and larger quantities of β precipitates which contribute less to the strength of the alloy due to their incoherency with the matrix [15, 16].

To prepare a billet of AA6082 for extrusion, it is homogenized at 570 °C for 6–18 h to dissolve any precipitates and homogenize the alloy before cooling it using forced air [17]. Just before the extrusion, the billet is reheated to below the solvus temperature of ~500 °C for hot forming [18]. During the extrusion, the heat generated by the deformation and friction increases the temperature of the workpiece above the solvus temperature between 500–530 °C [19]. This replaces the solution annealing usually required for the T6 temper. The extrudate is then quenched as it exits the die. The minimum recommended average cooling rate provided by AA6082 billet suppliers between the temperatures 500 °C and 300 °C is 2500 °C/min (~41 °C/s) to hold the Mg and Si in a supersaturated solution condition and prevent their depletion through undesired precipitation [20]. According to the minimum advised average cooling rate, the extrudate should cool from 500 °C to 300 °C in ~5 s or less. This means that the extrudate should be quenched immediately as it leaves the die before it air cools at lower cooling rates. Finally, the quenched extrudate is straightened, and cut to the required length before undergoing the desired aging treatment.

The extrudate is typically spray-quenched by a quench box placed close to the extrusion press to meet the recommended cooling rate. The quench box is equipped with multiple nozzles and quench zones spraying the pressurized coolant, typically water, with high impact speed on the surface of the extrudate [21–23]. The high pressure and speed of the coolant generate high heat flux out of the extrudate to cool it rapidly. However, multi-hollow profiles lead to the existence of interior walls that are not in direct contact with the coolant and limited paths for heat extraction. In addition to that, profiles are increasingly more complex and asymmetric. These characteristics are contrary to distortion reduction practices and therefore lead to great distortion problems as the profile is quenched [24–28]. This may result in extremely high part rejection rates and up to 40% scrap rates [29]. The cost of the reject extrusions can account for 26% of the cost per kilogram of acceptable extrusions as a result of wasted material, energy, labor, die wear, and time. In addition to that, the delays can cause strains on the extrusion plant, supply chain, and OEMs.

In this work, we will first demonstrate that using conventional spray quenching results in heterogeneous mechanical properties between external walls, where there is direct contact with the coolant, and the internal walls, where there is no direct contact with the coolant. Then we will demonstrate that using conventional spray quenching the cooling rate at the inner walls is significantly different than the external walls, which may explain the difference in the mechanical properties. Furthermore, we show, using automotive industry-relevant profiles, that for some multi-hollow profiles, conventional spray quenching cannot achieve the minimum recommended cooling rate at the inner walls of the profile regardless of the quenching heat transfer coefficient achieved on the external walls. Finally, we perform comparative computational case studies to present the potential impact simultaneous internal and external cooling can have on the cooling rates and quench distortion in contrast to conventional quenching.

The method of introducing the internal cooling to the inside walls of a multi-hollow profile is out of the scope of this article and will be illustrated in detail in future work. However, there are multiple examples in the literature showing the feasibility of manufacturing forging and extrusion dies with internal cooling channels [30–32]. The purpose of the extrusion die cooling channels in these papers was to prevent excessively heating the die during the extrusion process and preventing the extrudate from exceeding the recommended die exit temperatures which affects the surface quality [33, 34]. In [35, 36] it was shown that by using die conformal cooling, 30–50% higher extrusion speeds (ram speed) can be used without overheating the extrudate or the die. In this work, we demonstrate the potential benefits of extending the cooling channels into the hollow sections of the profile to provide direct cooling at the internal walls.

2 Methodology

2.1 Evaluating the Mechanical Properties of Hollow Extrusions Over the Cross-Section

A multi-hollow profile with current relevance to the automotive industry was chosen to demonstrate the effect of conventional quenching on the mechanical properties at different locations of the extrudate. The geometry and dimensions of the profile are illustrated in Fig. 1. The profile was press-quenched in a conventional spray quench box. Tensile specimens were extracted from different walls in the profile as shown in the right image of Fig. 1. The specimens were tested according to the ASTM E8/E8M standard.

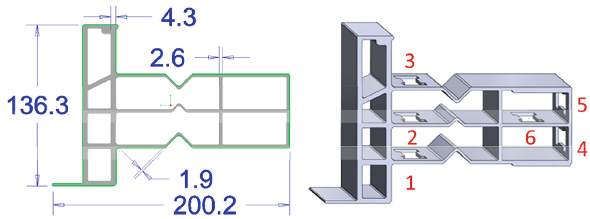

Fig. 1. Automotive AA6082 battery tray profile, the image on the left showing key dimensions (mm) and right image labeling the locations of the tensile specimens.

2.2 Thermal History of Conventionally Quenched Multi-hollow Profile

To demonstrate the different cooling rates sustained by the external walls and the interior walls of a multi-hollow profile, a 2D transient heat transfer FEA model was constructed for the automotive battery profile in Fig. 1. The simulation model was performed using ABAQUS 2022. The problem domain was defined as a 2D section with unit thickness. AA6082's key material properties are summarized in Table 1 and were extracted from the Deform 3D 13.0 material library. A transient heat transfer step was chosen to simulate the conventional spray quenching from 500 °C to room temperature. The temperature initial condition was specified as a predefined field and assigned 500 °C to the whole geometry. The spray quenching boundary condition was defined as an interaction surface film condition. The sink temperature, the temperature of the coolant, was defined as 25 °C. The film heat transfer coefficient was defined as 2000 W/m^2-K. The interaction film condition was assigned at the outer surface of the profile, which is highlighted by a green perimeter in Fig. 1. Quad-shaped mesh elements were selected. The global element size was defined as 0.20 mm. Local element sizes were defined for fine features such that no less than 14 elements were across the thickness of any wall and rounds were meshed by at least 8 elements.

A second model was constructed to demonstrate the impossibility of attaining the recommended minimum cooling rates at the internal walls using conventional quenching. In this model, spray quenching was modeled as an instantaneous 25 °C temperature boundary condition instead of a surface film interaction. The temperature boundary condition was assigned to the same outer perimeter highlighted in Fig. 1.

The logic behind choosing a surface film coefficient of 2000 W/m^2-K for the first simulation and an instantaneous 25 °C boundary condition for the second simulation is to encompass the range of feasible quenching rates. The 2000 W/m^2-K film coefficient is just high enough to cool the external walls at the recommended minimum cooling rate, while the instantaneous 25 °C boundary condition represents the upper cooling rate limit achievable using a coolant at room temperature. We show the futility of achieving the minimum cooling rate at the internal walls of the profile using conventional quenching by demonstrating it at both bounds of the quenching rate. Furthermore, we demonstrate that a significant temperature gradient will inevitably develop across the profile section regardless of the quenching rate.

Table 1. Material property definition for AA6082.

Property	Density	Specific Heat	Conductivity	Expansion Coefficient	Young's Modulus	Poisson's Ratio
Units	kg/m^3	J/kg-K	W/m-K	K^{-1}	Pa	–
AA6082	2660	896	198	2.2e−5	68.9e9	0.33

2.3 Coupled Thermo-mechanical Simulation of Conventional Quenching Compared to Simultaneous Quenching

In this section, we perform two comparative case studies using a simple, yet industry-relevant, multi-hollow profile. The profile's geometry and dimensions are illustrated in Fig. 2. This profile is quench sensitive due to its asymmetry and the thin internal wall dividing the two hollow sections. An aluminum extrusion plant reported that the profile is prone to bending and twisting as it quenches.

The first case study investigates the effect of conventional spray quenching on the quench distortion and residual stresses sustained by the profile after quenching. The second case study investigates the impact of introducing internal cooling on the inner walls of the profile, simultaneously with external cooling, on the quench distortion and residual stresses. The problem domain was defined as a deformable generalized plane strain 2D section with a uniform unit thickness. In addition to the material properties summarized in Table 1, temperature-dependent (25–500 °C) plastic stress-strain data were provided to the FEA model. The data were obtained from Deform 3D 13.0 material library for solution annealed AA6082. Table 2 lists key data points out of the 66 data points used to define the temperature-dependent plastic stress-strain curves.

The simulation is broken into three steps: the initial step, step 0, is used to define the initial condition temperature and mechanical boundary conditions, the heating step, step 1, is used to preheat the whole profile geometry to the die exit temperature of 500 °C uniformly, the cooling step, step 2, is used to define the quench surface film interaction. Implicit coupled temp-displacement (transient) steps were selected for steps 1 and 2.

The initial temperature for the whole profile was defined as 25 °C in step 0 as a predefined field. The purpose of defining the initial temperature as 25 °C instead of 500 °C is to compare the deformation of the quenched profile at the end of the simulation using the same reference temperature. Mechanical boundary conditions are applied, according to jig theory for free-floating models, in step 0 and remain active throughout the simulation (see Fig. 2). In step 1, the temperature is increased from 25 °C to 500 °C throughout the profile uniformly in one second. Due to the uniform expansion, this step does not contribute to the residual stresses (less than 6×10^{-12} of the lowest yield strength). In step 2, the spray quench cooling effect is defined as a surface film interaction with sink temperature (cooling fluid temperature) of 25 °C and a film heat transfer coefficient of 2000 W/m^2-K. For the conventional spray quench model, the surface film interaction is applied on the outer perimeter of the profile as highlighted by the red box in Fig. 2. For the simultaneous internal and external cooling model, the surface film interaction is applied on the walls highlighted in blue as well as the red box. The inner side of the left wall was chosen due to its larger thickness compared to the other walls. One side of the middle wall was selected due to the absence of direct contact with the coolant in conventional spray quenching. Coupled temperature-displacement elements were selected for generalized plane strain analysis. Only quad elements were used. The simulations were repeated for global element sizes of 0.4, 0.2, and 0.1 mm to confirm the results' independence of the mesh size.

Table 2. Key temperature-dependent plastic stress-strain data.

Temperature (C)	25	25	300	300	500	500
Plastic Strain (mm/mm)	0	0.1	0	0.1	0	0.1
Flow stress (MPa)	87.6	89.2	68.9	76.5	37.2	37.2

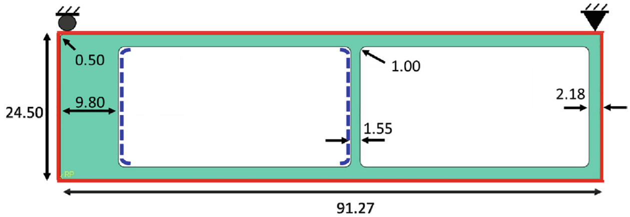

Fig. 2. Cross section of the simple quench sensitive profile highlighting the external quench surface in red, the internal quench surface in blue, and key dimensions (mm) (Color figure online).

3 Results and Discussion

3.1 Results of the Mechanical Properties Evaluation Over the Cross-Section

The tensile tests' engineering stress-strain curves and the locations of the tensile specimens are illustrated in Fig. 3. The curves show a clear distinction between specimens extracted from external walls compared to specimens extracted from inner walls. The average strain before fracture for the external walls is 0.085 mm/mm compared to the 0.062 mm/mm average fracture strain for specimens extracted from the inner walls. The external walls have a 36% larger fracture strain compared to the inner walls. Furthermore, the average ultimate tensile strength for the external wall is 337 MPa compared to 318 MPa for the inner walls, which represents a 6% increase. The discrepancy can be explained by the cooling rate difference as shall be demonstrated in the following section.

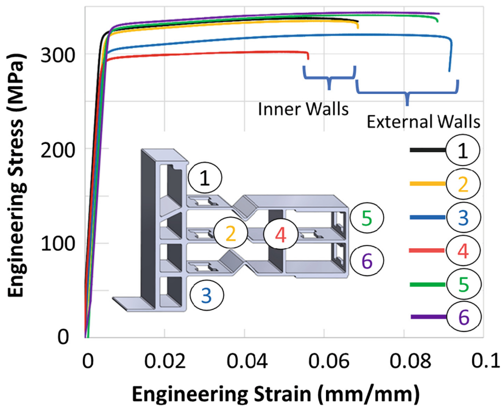

Fig. 3. Tensile test results

3.2 Thermal History and Contours of Conventionally Quenched Multi-hollow Profile

The results of the transient heat transfer simulations of conventionally quench multi-hollow profiles are illustrated in Fig. 4. From the top panels, we can see that for a heat transfer coefficient of 2000 W/m^2-K, the cooling rate of the external walls between 500 °C and 300 °C is above the minimum recommended cooling rate. The internal wall however takes an additional 20 s to reach 300 °C. The temperature contours after 5 s of cooling reveal that a significant region of the internal walls is still above 300 °C. This means that the cooling rate for these regions is below the recommended 41 °C/s (8.7 °C/s for this heat transfer coefficient). We performed similar simulations for heat transfer coefficients ranging 500–1,000,000 W/m^2-K. The resulting cooling rates for the internal wall were 5.7–12.3 °C/s. Furthermore, the bottom panels of Fig. 4 show that even if the external surface of the walls were cooled instantaneously from 500 °C to 25 °C, the center of the profile is still not cooling at the minimum recommended rate. The contours reveal that, while slightly smaller than the surface film condition simulation, the region with temperatures above 300 °C after 5 s of cooling is significantly large. The temperature history of the center of the profile shows that cooling rates above 12.4 °C/s are impossible at the center of this profile regardless of the heat transfer coefficients attained on the external wall. The simulations were repeated using different mesh sizes and using linear and quad elements. The results proved to be mesh independent. The cooling rates and temperature contours approach those of the instantaneously cooled boundary simulation as the heat transfer coefficient increases from 500–1,000,000 W/m^2-K, thus demonstrating that the results of the instantaneously cooled boundary simulation are trustworthy.

The difference between the cooling rates at the external walls and the internal regions can be a major factor in the different mechanical properties measured at different sections of the profile. Furthermore, the temperature gradient between the external and interior regions of the profile are significant regardless of the quenching rate and will result in uneven thermal expansion and distortion.

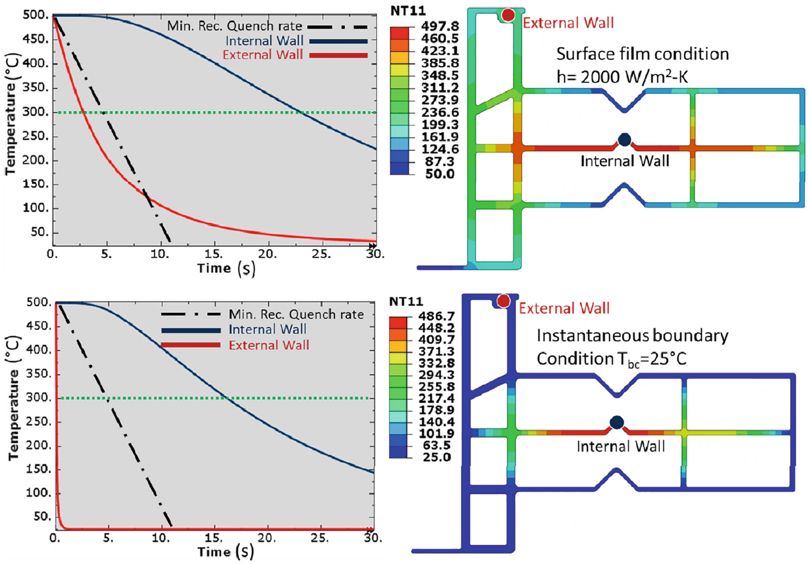

Fig. 4. Thermal history of a point on the external wall and a point on the inner wall, and temperature contours after 5 s of cooling. Top panels showing results for surface film condition and bottom images showing results for instantaneous boundary condition.

3.3 Results of Coupled Thermo-mechanical Simulation Case Studies

The results of the coupled thermo-mechanical simulations are summarized in Figs. 5 and 6. The von Mises stress and equivalent plastic strain fields are reported for time steps in which the profile has cooled to room temperature in both simulations. For conventional cooling, we can see from Fig. 5 that the internal middle wall sustains significant residual stresses. The center of that wall carries stresses (57 MPa) larger than half of AA6082 yield strength at room temperature (87.6 MPa). The presence of plastic strains signifies that the von Mises stresses exceeded the yield strength during cooling. Due to non-uniform cooling and uneven thermal expansion, the middle wall experiences compressive stresses as the external walls cool faster. The middle wall is plastically compressed when the stresses exceed the yield strength. Due to the small thickness of the middle wall, it could be prone to buckling. As the middle wall cools, it shrinks and starts to experience tensile stresses from the external walls. Furthermore, the internal side of the thick left wall shows slight plastic deformation because it cools later than the outer side of the left wall. The delay in cooling the internal side of the left wall compared to the external side induced stresses greater than the yield strength. This is due to the large thermal inertia of the left wall caused by its thickness.

For simultaneous external and internal cooling, the profile sustained significantly lower residual stresses compared to conventional quenching (see Fig. 6). The maximum von Mises stress sustained by the simultaneously cooled profile is 3 orders of magnitude smaller than the conventionally quenched profile. The equivalent plastic strain field indicated zero plastic deformation throughout the profile. This signifies that the cooling was uniform enough to prevent uneven expansion from inducing stresses larger than the yield strength at any point during the cooling process from 500 °C to 25 °C. It should be noted that the choice of the locations where the internal cooling was applied was inspired by the plastic strain field from the conventional quenching simulation.

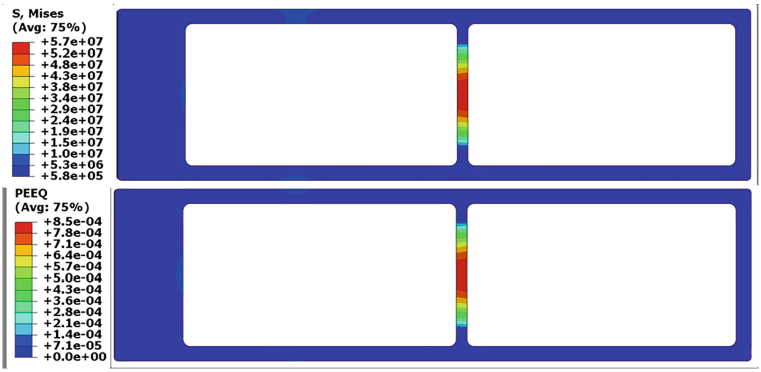

Fig. 5. von Mises stress (S, Mises) field and equivalent plastic strain (PEEQ) field for conventionally quenched profile.

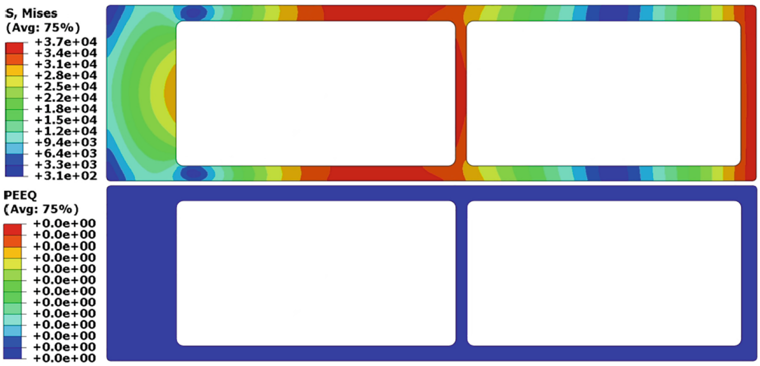

Fig. 6. von Mises stress (S, Mises) field and equivalent plastic strain (PEEQ) field for simultaneous external and internal cooling.

4 Conclusions and Future Work

Lightweighting has driven automotive OEMs to pursue thinner walls, more complex, and more hollow AA6082 extrusion profiles. The dependence of the mechanical properties on the press-quench cooling rates led aluminum extrusion plants to apply high-pressure spray quenching to achieve a high cooling rate and maximize the structural efficiency of the extrusions. In this work, we evaluate the mechanical properties across the section of a multi-hollow profile by extracting tensile specimens from different locations. Heat transfer and thermo-mechanical FEA models were developed to estimate the thermal history, residual stresses, and plastic strain of industry-relevant multi-hollow profiles during press-quenching. A case study was performed demonstrating the potential advantages of extending cooling to the internal surfaces of a multi-hollow profile. The results reveal the following:

- The tensile strength and ductility of conventionally quenched multi-hollow profiles are significantly superior (higher) at the external walls compared to the inner walls, where no direct contact with coolant is present.
- The difference in the mechanical properties can be explained by the different cooling rates experienced by different regions throughout the profile. The external walls sustain rapid cooling rates due to their proximity to the convection surface. The heat from the internal walls has to be extracted through conductivity through thin walls which causes lower cooling rates.
- The need for internal cooling for thin-walled multi-hollow profiles is evident. The instantaneously cooled boundary condition simulation revealed that it is impossible to achieve the recommended minimum cooling rate at the inner regions of the thin-walled multi-hollow profile regardless of the magnitude of the heat transfer coefficient achieved on the external surface. The cooling rate of the inner regions depends on the thermal conductivity and the geometry of the profile.
- By providing simultaneous external and internal cooling, the profile can be cooled more evenly which reduces the residual stresses by several orders of magnitude and eliminates quench distortion. This can reduce the extrusion rejects due to quench distortion and reduce the cost of material, energy, and labor. Furthermore, by achieving similar cooling rates at the internal surfaces as the external surfaces, the mechanical properties are expected to improve.
- Replicating the simulation cooling effect on the interior surfaces in an experimental setup is expected to be challenging, especially targeting the selected areas exclusively. However, an experimental cooling system inspired by the simulation cooling effect is expected to produce more uniform profile cooling than conventional quenching, even if it does not reproduce the exact average heat transfer coefficient (the simulations predict similar results for 0.5–2$\times$ the heat transfer coefficient used in the reported simulation). Thus, significant reduction in the residual stresses, and quench distortion, in addition to improvement in the mechanical properties is still achievable.
- In future work, we will present the method of providing the internal cooling through the die mandrel to the hollow section of the extrusion profile. Furthermore, we will experimentally demonstrate the impact of simultaneous internal and external cooling on the cooling rate, residual stresses, and plastic deformation.

- By assuming generalized plane strain during the coupled thermo-mechanical FEA simulation, the model assumes constant temperature, stress, and strain through the length of the profile (out-of-plane axis). In future work, we use a deformable 3D FEA model and a moving surface film interaction. This model will be able to simulate the profile as it enters the quench box and estimate temperature variations along the length of the profile, out of plane shear stress components, and bending and twisting deformations.

References

1. Mordor Intelligence. Automotive Aluminium Extrusion Market Analysis – Industry Report – Trends, Size & Share. https://www.mordorintelligence.com/industry-reports/automotive-aluminium-extrusion-market. Accessed 06 Feb 2023
2. Liang, R., Liu, X., Hu, Y., Jiang, C., Bastien, C.: A methodology to investigate and optimise the crashworthiness response of foam-filled twelve right angles thin-walled structures under axial impact. Compos. Struct. **310**, 116736 (2023)
3. Gribniak, V., Rimkus, A., Misiūnaitė, I., Zakaras, T.: Improving local stability of aluminium profile with low-modulus stiffeners: experimental and numerical web buckling analysis. Thin-Walled Struct. **172**, 108858 (2022)
4. Ashkenazi, D.: How aluminum changed the world: a metallurgical revolution through technological and cultural perspectives. Technol. Forecast. Soc. Change **143**, 101–113 (2019)
5. I. J. Polmear, "Solute partitioning to enhance mechanical properties of aged aluminium alloys," *Fundam. Alum. Metall. Prod. Process. Appl.*, pp. 367–385, Jan. 2011
6. The Aluminum Association: Aluminum standards and data. Standards **3**, 1–216 (1993)
7. Parson, N.C., et al.: Effect of press quench rate on automotive extrusion performance. In: Proceedings of Twelfth International Aluminum Extrusion Technology Seminar, pp. 1–19
8. Aluminium Alloy – Commercial Alloy – 6082 – T6~T651 Plate. https://www.aalco.co.uk/datasheets/Aluminium-Alloy_6082-T6~T651_148.ashx. Accessed 03 Mar 2023
9. Aluminium 6082: Properties, Fabrication and Applications. https://www.azom.com/article.aspx?ArticleID=2813. Accessed 03 Mar 2023
10. Hua, L., Yuan, P.G., Zhao, N., Hu, Z.L., Ma, H.J.: Microstructure and mechanical properties of 6082 aluminum alloy processed by preaging and hot forging. Trans. Nonferrous Met. Soc. China **32**(3), 790–800 (2022)
11. Lai, Y.X., Jiang, B.C., Liu, C.H., Chen, Z.K., Wu, C.L., Chen, J.H.: Low-alloy-correlated reversal of the precipitation sequence in Al-Mg-Si alloys. J. Alloys Compd. **701**, 94–98 (2017)
12. Lai, Y.X., Fan, W., Yin, M.J., Wu, C.L., Chen, J.H.: Structures and formation mechanisms of dislocation-induced precipitates in relation to the age-hardening responses of Al-Mg-Si alloys. J. Mater. Sci. Technol. **41**, 127–138 (2020)
13. Wang, X.D., et al.: Microstructure and mechanical properties of Al−Mg−Si alloy U-shaped profile. Trans. Nonferrous Met. Soc. China **30**(11), 2915–2926 (2020)
14. Zhao, N., et al.: Microstructural evolutions and mechanical properties of 6082 aluminum alloy part produced by a solution-forging integrated process. J. Mater. Process. Technol. **308**, 117715 (2022)
15. Jadhav, S., Singh, R., Pawar, V., Mane, S.: Influence of heat treatment on mechanical properties and microstructure of en AW 6082 aluminum alloy. In: 2017 8th International Conference on Mechanical and Aerospace Engineering. ICMAE 2017, pp. 184–187 (2017)

16. Marioara, C.D., Andersen, S.J., Zandbergen, H.W., Holmestad, R.: The influence of alloy composition on precipitates of the Al-Mg-Si system. Metall. Mater. Trans. A **36**(3), 691–702 (2005). https://doi.org/10.1007/s11661-005-0185-1
17. Zyna Mrówka-Nowotnik, G., Sieniawski, J.: Influence of heat treatment on the microstructure and mechanical properties of 6005 and 6082 aluminium alloys. J. Mater. Process. Technol. **162**, 367–372 (2005).https://doi.org/10.1016/j.jmatprotec.2005.02.115
18. Wang, D.G., Shu, X.D., Wang, R., Xu, S.: Mechanism of necking defect of 6082 aluminium alloy rolled by cross-wedge rolling method based on material thermal properties. J. Cent. South Univ. **27**(12), 3721–3732 (2020)
19. Y. Birol and O. Ilgaz: Effect of cast and extruded stock on grain structure of EN AW 6082 alloy forgings. Mater. Sci. Technol. **30**(7), 860–866, 2014. https://doi.org/10.1179/1743284713Y.0000000407
20. Griffioen, D.T., Clark, G.: Measuring Instantaneous Extrusion Quench Performance. In: Proceedings of Twelfth International Aluminum Extrusion Technology Seminar, pp. 1–8
21. Jenista, D., Victor, J., Nickolopoulos, N.: The effect of water temperature on quench rates do 400 and 290 C represent the extrusion and quenching temperatures of. In: Proceedings of Twelfth International Aluminum Extrusion Technology Seminar, pp. 1–6
22. Zhou, N., Chen, F., Cao, Y., Chen, M., Wang, Y.: Experimental investigation on the performance of a water spray cooling system. Appl. Therm. Eng. **112**, 1117–1128 (2017)
23. Cebo-Rudnicka, A., Malinowski, Z., Buczek, A.: The influence of selected parameters of spray cooling and thermal conductivity on heat transfer coefficient. Int. J. Therm. Sci. **110**, 52–64 (2016)
24. Yang, Y.P., Dong, P.: Buckling distortions and mitigation techniques for thin-section structures. J. Mater. Eng. Perform. **21**(2), 153–160 (2012)
25. Dong, P.: Residual stresses and distortions in welded structures: a perspective for engineering applications. Sci. Technol. Weld. Join. **10**(4), 389–398 (2013). https://doi.org/10.1179/174329305X29465
26. Bikass, S., Andersson, B., Pilipenko, A., Langtangen, H.P.: Simulation of the distortion mechanisms due to non-uniform cooling in the aluminum extrusion process. Int. J. Therm. Sci. **52**(1), 50–58 (2012)
27. Xue, X., Liao, J., Vincze, G., Gracio, J.J.: Modelling of mandrel rotary draw bending for accurate twist springback prediction of an asymmetric thin-walled tube. J. Mater. Process. Technol. **216**, 405–417 (2015)
28. Li, Z.X., Zhan, M., Fan, X.G., Wang, X.X., Ma, F., Li, R.: Multi-mode distortion behavior of aluminum alloy thin sheets in immersion quenching. J. Mater. Process. Technol. **279**, 116576 (2020)
29. Oberhausen, G., Zhu, Y., Cooper, D.R.: Reducing the environmental impacts of aluminum extrusion. Resour. Conserv. Recycl. **179**, 106120 (2022)
30. Tan, C., et al.: Design and additive manufacturing of novel conformal cooling molds. Mater. Des. **196**, 109147 (2020)
31. Behrens, B.-A., Bouguecha, A., Vucetic, M., Bonhage, M., Malik, I.Y.: Numerical investigation for the design of a hot forging die with integrated cooling channels. Procedia Technol. **26**, 51–58 (2016)
32. Stratton, P.: Raising productivity of aluminium extrusion with nitrogen. Int. Heat Treat. Surf. Eng. **2**(3–4), 105–108 (2013). https://doi.org/10.1179/174951508X429221
33. Hölker, R., Tekkaya, A.E.: Advancements in the manufacturing of dies for hot aluminum extrusion with conformal cooling channels. Int. J. Adv. Manuf. Technol. **83**(5–8), 1209–1220 (2015). https://doi.org/10.1007/s00170-015-7647-4
34. Reggiani, B., Todaro, I.: Investigation on the design of a novel selective laser melted insert for extrusion dies with conformal cooling channels. Int. J. Adv. Manuf. Technol. **104**(1–4), 815–830 (2019). https://doi.org/10.1007/s00170-019-03879-9

35. Pelaccia, R., Negozio, M., Donati, L., Reggiani, B., Tomesani, L.: Efficiency of conformal cooling channels inserts for extrusion dies. Procedia Manuf. **47**, 209–216 (2020)
36. Hölker, R., Haase, M., Ben Khalifa, N., Tekkaya, A.E.: Hot extrusion dies with conformal cooling channels produced by additive manufacturing. Mater. Today Proc. **2**(10), 4838–4846 (2015)